atmosphere

MDPI

Supplementary Materials: Analysis of MONARC and ACTIVATE Airborne Aerosol Data for Aerosol-Cloud Interaction Investigations: Efficacy of Stairstepping Flight Legs for Airborne in situ Sampling

Hossein Dadashazar [1,*], Ewan Crosbie [2,3], Yonghoon Choi [2,3], Andrea F. Corral [1], Joshua P. DiGangi [2], Glenn S. Diskin [2], Sanja Dmitrovic [4], Simon Kirschler [5,6], Kayla McCauley [7], Richard H. Moore [2], John B. Nowak [2], Claire E. Robinson [2,3], Joseph Schlosser [1], Michael Shook [2], Kenneth Lee Thornhill [2], Christiane Voigt [5,6], Edward L. Winstead [2,3], Luke D. Ziemba [2] and Armin Sorooshian [1,4,7,*]

S1. Comparison of Adjacent Below Cloud Base Legs in ACTIVATE

One aspect in the design of ACTIVATE was to split BCB and ACB legs in half such that they alternate and are ~3 min each rather than keeping one of each at ~6 min duration. This change in duration allows for an examination of horizontal variability to see how much variables vary between legs in each BCB pair. Table S7 summarizes quantities associated with adjacent BCB legs including variable values and degree of similarity, along with correlation and slope statistics. Representative scatterplots are in Figure S4. The average horizontal distance between the end of the first BCB and beginning of next BCB was 56 km. The median altitudes for two BCB legs were 777 and 809 m. At times, a BCB leg's altitude had to be modified relative to the previous one to adjust for cloud base height variability. As the altitudes were similar, any significant disagreement for variable values between two BCB legs is largely attributed to the differences in horizontal gradients and/or the intrinsic uncertainties in the measurements.

Potential temperature exhibited the highest correlation among variables (R^2 = 0.99), with a slope of 0.98 and high similarity of values between adjacent BCB legs (MARD = 0.00). Little difference was observed between winter and summer seasons. Concentrations of gases were highly correlated ($R^2 \geq 0.89$) with slopes of 0.93–0.99 and the highest similarity (MARD ≤ 0.07) among all variables excluding θ. General trends for aerosol number concentrations were the same as the BCB/Min. Alt. analysis in Section 3.1 with a notable exception being that the slopes of the $N_{a>3nm}$ and $N_{a>10nm}$ variables were now more similar to the other aerosol variables (0.76 and 0.81, respectively) without any major seasonal difference. This could point to the vertical inhomogeneity in where new particle formation events occur, which is no longer an issue for adjacent BCB legs that are at the same level.

In terms of AMS composition data, organics and sulfate were strongly correlated between BCB legs for both seasons ($R^2 \geq 0.83$) with the exception of organics in winter owing to presumed offshore flow leading to a strong organic gradient in contrast to sulfate that has more influence of sources over the ocean. Slopes were 0.81–0.95. Both wind and σ_{wind} exhibited high correlations (R^2: 0.74–0.89) and similarity (MARD: 0.14–0.20) between adjacent BCB legs, without major differences between seasons.

Table S1. Statistics for selected aerosol, gaseous, and meteorological variables measured during the pair of two BCB legs in each cloud ensemble of MONARC 2019 flights.

(Min. Alt./BCB)/(Min. Alt./BBL)

Parameter	Min	25th percentile	75th percentile	Max	no. pairs
Altitude (m)	(27/55)/(28/90)	(31/158)/(31/166)	(152/279)/(33/199)	(702/770)/(104/575)	31/30
$N_{a,>3nm}$ (cm^{-3})	(31/39)/(403/417)	(92/99)/(831/761)	(805/564)/(1932/1784)	(1744/1041)/(8315/7845)	23/26
$N_{a,>10nm}$ (cm^{-3})	(25/33)/(338/357)	(80/86)/(578/617)	(684/479)/(878/932)	(1282/885)/(5152/4506)	23/26
$N_{a,127-901nm}$ (cm^{-3})	(9/8)/(69/68)	(36/29)/(104/109)	(213/186)/(187/168)	(595/559)/(732/619)	23/26
$N_{a,>901nm}$ (cm^{-3})	(0.00/0.04)/(0.98/0.47)	(0.41/0.39)/(1.75/1.05)	(1.72/1.11)/(2.88/2.56)	(2.82/1.96)/(4.35/3.78)	23/26
$N_{a,>3270nm}$ (cm^{-3})	(0.09/0.16)/(0.00/0.00)	(0.69/1.01)/(0.58/0.49)	(1.12/2.76)/(1.37/1.48)	(4.01/6.61)/(1.81/6.15)	23/26
H_2O ($g\ kg^{-1}$)	(5.9/5.2)/(6.5/3.5)	(8.1/8.0)/(7.1/6.5)	(9.0/8.8)/(8.1/7.7)	(9.5/9.6)/(10.7/10.5)	31/30
wind ($m\ s^{-1}$)	(2.5/3.5)/(1.9/1.5)	(8.6/9.6)/(6.2/10.2)	(13.7/15.2)/(12.9/16.1)	(19.8/21.4)/(15.1/18.6)	31/30
σ_{wind} ($m\ s^{-1}$)	(0.2/0.1)/(0.1/0.0)	(0.4/0.3)/(0.3/0.2)	(0.6/0.5)/(0.7/0.6)	(0.8/0.8)/(1.0/0.8)	31/30
θ (K)	(283.6/283.8)/(283.6/283.9)	(284.4/284.6)/(284.7/284.8)	(285.5/286.0)/(285.8/286.3)	(286.6/287.4)/(293.1/296.7)	31/30

Table S2. Statistics for selected aerosol, gaseous, and meteorological variables measured during adjacent Min. Alt./BCB legs and Min. Alt./BBL legs for cloud and clear ensembles, respectively, for ACTIVATE 2020 flights.

(Min. Alt./BCB)/(Min. Alt./BBL)

Parameter	Min	25th percentile	75th percentile	Max	no. pairs
Altitude (m)	(103/129)/(111/258)	(115/458)/(116/342)	(123/954)/(125/793)	(144/1430)/(193/1087)	111/54
$N_{a,>3nm}$ (cm^{-3})	(230/284)/(613/426)	(925/829)/(1772/1471)	(2349/2241)/(4634/4628)	(11338/7058)/(15654/28117)	111/54
$N_{a,>10nm}$ (cm^{-3})	(190/228)/(515/361)	(749/653)/(1465/1205)	(1937/1830)/(3675/3752)	(8277/5404)/(11632/14526)	111/54
$N_{a,100-1000nm}$ (cm^{-3})	(34/41)/(106/46)	(178/176)/(296/288)	(472/423)/(761/678)	(1319/1414)/(1478/1289)	111/54
$N_{a,>1000nm}$ (cm^{-3})	(0.17/0.15)/(0.08/0.11)	(0.58/0.57)/(0.40/0.29)	(1.42/1.43)/(1.10/0.84)	(4.92/3.94)/(2.74/2.24)	111/54
$N_{a,>3000nm}$ (cm^{-3})	(0.06/0.04)/(0.01/0.01)	(0.21/0.25)/(0.11/0.08)	(0.45/0.82)/(0.33/0.28)	(1.18/4.36)/(0.74/1.11)	106/48
Organic ($\mu g\ m^{-3}$)	(0.02/0.03)/(0.03/0.07)	(0.43/0.44)/(1.18/1.20)	(1.91/1.79)/(5.58/5.68)	(16.84/17.77)/(16.10/10.09)	111/53
Sulfate ($\mu g\ m^{-3}$)	(0.18/0.16)/(0.16/0.10)	(0.58/0.54)/(0.72/0.68)	(1.22/1.44)/(1.58/1.52)	(4.08/3.87)/(3.65/3.53)	111/53
CH_4 (ppb)	(1884/1884)/(1898/1891)	(1953/1953)/(1963/1963)	(1993/1988)/(2016/2003)	(2032/2028)/(2142/2132)	111/54
CO_2 (ppm)	(401.3/399.8)/(400.4/399.1)	(407.9/406.2)/(411.3/410.7)	(419.9/419.5)/(421.7/421.0)	(425.9/425.4)/(430.8/431.1)	111/54
CO (ppb)	(64.6/66.8)/(72.8/72.9)	(107.0/104.2)/(127.0/125.9)	(138.7/139.9)/(147.8/146.0)	(164.4/158.9)/(195.8/203.2)	111/54
O_3 (ppb)	(17.8/13.9)/(21.8/16.3)	(33.9/33.8)/(40.8/41.5)	(45.0/45.3)/(47.8/50.0)	(52.8/54.5)/(59.0/62.6)	110/54
H_2O (ppm)	(3227/2516)/(2932/1341)	(7143/6784)/(6843/4229)	(20364/20000)/(23167/18051)	(32691/34195)/(30279/29001)	111/53
wind ($m\ s^{-1}$)	(2.7/1.7)/(2.3/1.3)	(6.4/5.8)/(5.2/4.3)	(10.5/11.0)/(8.7/8.1)	(21.7/21.3)/(12.9/13.6)	109/54
σ_{wind} ($m\ s^{-1}$)	(0.1/0.1)/(0.1/0.1)	(0.5/0.5)/(0.4/0.2)	(1.0/0.9)/(0.7/0.5)	(1.9/1.7)/(1.1/1.2)	111/53
θ (K)	(270.4/272.7)/(273.6/273.8)	(283.8/284.2)/(280.4/282.1)	(296.0/296.5)/(296.5/297.2)	(301.2/301.3)/(300.1/303.0)	111/54

Table S3. Statistics for the absolute value of the variable slopes measured during adjacent Min. Alt./BCB legs and Min. Alt./BBL legs for cloud and clear ensembles, respectively, for MONARC 2019 flights.

	(Min. Alt./BCB)/(Min. Alt./BBL)			
Parameter	Min	25^{th} percentile	75^{th} percentile	Max
$N_{a,>3nm}$ (cm^{-3} km^{-1})	(0.24/0.16)/(0.11/0.17)	(0.97/1.04)/(2.35/5.07)	(7.71/5.46)/(17.09/16.96)	(35.76/145.5)/(1163.54/872.50)
$N_{a,>10nm}$ (cm^{-3} km^{-1})	(0.25/0.04)/(0.24/0.15)	(1.45/0.72)/(1.64/3.84)	(6.53/4.38)/(13.59/17.63)	(29.21/118.45)/(690.02/520.65)
$N_{a,127-901nm}$ (cm^{-3} km^{-1})	(0.02/0.06)/(0.01/0.00)	(0.18/0.32)/(0.23/0.23)	(0.98/1.34)/(1.04/1.52)	(10.56/3.59)/(54.74/12.83)
$N_{a,>901nm}$ (cm^{-3} km^{-1})	(0.0013/0.0013)/(0.0003/0.0040)	(0.0054/0.0086)/(0.0049/0.0104)	(0.0427/0.0788)/(0.0187/0.0361)	(0.1789/0.2261)/(0.1610/0.0603)
$N_{a,>3270nm}$ (cm^{-3} km^{-1})	(0.0003/0.0008)/(0.0001/0.0000)	(0.0078/0.0326)/(0.0029/0.0026)	(0.0555/0.2772)/(0.0165/0.0364)	(10.5203/1.5844)/(0.0907/0.1882)
H_2O (g kg^{-1} km^{-1})	(0.00/0.00)/(0.00/0.00)	(0.00/0.00)/(0.00/0.00)	(0.01/0.02)/(0.02/0.02)	(0.02/0.10)/(0.31/0.30)
wind (m s^{-1} km^{-1})	(0.001/0.000)/(0.003/0.003)	(0.011/0.019)/(0.015/0.024)	(0.063/0.065)/(0.101/0.098)	(0.184/0.559)/(0.343/0.377)
θ (K km^{-1})	(0.000/0.000)/(0.000/0.000)	(0.002/0.003)/(0.002/0.004)	(0.012/0.017)/(0.017/0.020)	(0.028/0.117)/(0.190/0.126)

Table S4. Statistics for the standard deviation of variable values measured in cloud and clear legs during MONARC 2019 flights.

(Min. Alt./BCB)/(Min. Alt./BBL)

Parameter	Min	25th percentile	75th percentile	Max
$N_{a,>3nm}$ (cm^{-3})	(4/12)/(33/23)	(16/26)/(50/44)	(47/57)/(117/123)	(695/703)/(2070/4239)
$N_{a,>10nm}$ (cm^{-3})	(3/5)/(5/4)	(9/10)/(7/10)	(24/31)/(83/73)	(520/571)/(1004/1829)
$N_{a,127\text{-}901nm}$ (cm^{-3})	(4/4)/(9/9)	(7/7)/(11/11)	(18/19)/(14/14)	(58/31)/(69/96)
$N_{a,>901nm}$ (cm^{-3})	(0.51/0.20)/(0.96/0.75)	(1.12/0.94)/(1.37/1.06)	(1.67/1.89)/(1.83/1.67)	(5.25/4.24)/(2.31/2.17)
$N_{a,>3270nm}$ (cm^{-3})	(0.22/0.76)/(0.20/0.10)	(0.27/0.76)/(0.23/0.23)	(0.45/1.05)/(0.33/0.51)	(0.64/1.64)/(0.55/0.63)
H_2O ($g\ kg^{-1}$)	(0.0/0.0)/(0.0/0.0)	(0.0/0.0)/(0.0/0.1)	(0.1/0.1)/(0.1/0.1)	(0.1/0.6)/(0.6/0.3)
wind ($m\ s^{-1}$)	(0.3/0.3)/(0.1/0.1)	(0.5/0.4)/(0.3/0.2)	(0.8/0.7)/(0.8/0.7)	(1.2/1.1)/(1.0/1.3)
θ (K)	(0.0/0.0)/(0.0/0.0)	(0.1/0.1)/(0.0/0.0)	(0.1/0.1)/(0.1/0.1)	(0.1/0.3)/(0.3/0.3)

Table S5. Statistics for the absolute value of the variable slopes measured in cloud and clear legs during ACTIVATE 2020 flights.

(Min. Alt./BCB)/(Min. Alt./BBL)

Parameter	Min	25th percentile	75th percentile	Max
$N_{a,>3nm}$ (cm^{-3} km^{-1})	(0.03/0.01)/(0.12/0.00)	(1.69/1.78)/(5.02/3.68)	(12.07/12.5)/(39.72/44.18)	(266.64/234.59)/(503.99/521.92)
$N_{a,>10nm}$ (cm^{-3} km^{-1})	(0.03/0.05)/(0.15/0.27)	(1.32/1.58)/(4.21/3.14)	(9.26/9.49)/(26.81/29.92)	(184.31/177.54)/(393.12/343.72)
$N_{a,100-1000nm}$ (cm^{-3} km^{-1})	(0.00/0.00)/(0.02/0.01)	(0.56/0.49)/(0.45/0.92)	(2.28/2.58)/(3.01/4.00)	(11.83/27.28)/(8.19/32.00)
$N_{a,>1000nm}$ (cm^{-3} km^{-1})	(0.0001/0.0002)/(0.0001/0.0003)	(0.0037/0.0046)/(0.0026/0.0021)	(0.0163/0.0184)/(0.0147/0.0132)	(0.1132/0.3108)/(0.0777/0.0633)
$N_{a,>3000nm}$ (cm^{-3} km^{-1})	(0.0000/0.0000)/(0.0003/0.0000)	(0.0007/0.0015)/(0.0011/0.0006)	(0.0045/0.0106)/(0.0051/0.0055)	(0.0240/0.1289)/(0.0169/0.0782)
Organic ($\mu g\ m^{-3}$ km^{-1})	(0.0002/0.0001)/(0.0000/0.0004)	(0.0055/0.0040)/(0.0074/0.0070)	(0.0222/0.0251)/(0.0308/0.0335)	(0.1303/0.1034)/(0.0698/0.1359)
Sulfate ($\mu g\ m^{-3}$ km^{-1})	(0.0001/0.0000)/(0.0000/0.0001)	(0.0018/0.0016)/(0.0023/0.0014)	(0.0091/0.0092)/(0.0086/0.0068)	(0.0310/0.0393)/(0.0546/0.0284)
CH_4 (ppb km^{-1})	(0.00/0.00)/(0.00/0.01)	(0.03/0.02)/(0.05/0.07)	(0.16/0.18)/(0.42/0.40)	(1.10/1.28)/(49.46/1.01)
CO_2 (ppm km^{-1})	(0.000/0.000)/(0.000/0.001)	(0.004/0.005)/(0.005/0.005)	(0.019/0.021)/(0.047/0.034)	(0.197/0.101)/(9.285/0.222)
CO (ppb km^{-1})	(0.000/0.001)/(0.003/0.006)	(0.034/0.026)/(0.046/0.041)	(0.124/0.116)/(0.216/0.175)	(0.577/0.538)/(3.087/0.774)
O_3 (ppb km^{-1})	(0.000/0.001)/(0.001/0.002)	(0.018/0.017)/(0.027/0.017)	(0.061/0.059)/(0.106/0.076)	(0.266/1.774)/(0.949/0.341)
H_2O (ppm km^{-1})	(0.76/0.19)/(0.76/0.83)	(9.92/8.49)/(9.53/6.49)	(37.26/35.14)/(35.25/76.98)	(139.46/210.84)/(160.70/282.90)
wind ($m\ s^{-1}$ km^{-1})	(0.000/0.000)/(0.000/0.000)	(0.011/0.013)/(0.014/0.018)	(0.053/0.058)/(0.052/0.056)	(0.220/0.235)/(0.325/0.135)
θ (K km^{-1})	(0.000/0.000)/(0.000/0.001)	(0.004/0.004)/(0.003/0.006)	(0.017/0.017)/(0.022/0.022)	(0.080/0.176)/(0.062/0.064)

Table S6. Statistics for the standard deviation of variable values measured in cloud and clear legs during ACTIVATE 2020 flights.

(Min. Alt./BCB)/(Min. Alt./BBL)

Parameter	Min	25th percentile	75th percentile	Max
$N_{a,>3nm}$ (cm^{-3})	(21/22)/(27/21)	(50/58)/(76/68)	(150/160)/(326/452)	(1283/1337)/(2225/2060)
$N_{a,>10nm}$ (cm^{-3})	(6/6)/(8/5)	(15/27)/(36/42)	(102/101)/(188/280)	(857/856)/(1018/1565)
$N_{a,100-1000nm}$ (cm^{-3})	(7/9)/(12/11)	(18/19)/(22/25)	(39/39)/(47/48)	(98/198)/(194/241)
$N_{a,>1000nm}$ (cm^{-3})	(0.43/0.39)/(0.30/0.35)	(0.76/0.80)/(0.69/0.59)	(1.31/1.42)/(1.14/1.00)	(2.01/5.64)/(6.28/1.52)
$N_{a,>3000nm}$ (cm^{-3})	(0.04/0.04)/(0.03/0.02)	(0.10/0.13)/(0.08/0.08)	(0.16/0.29)/(0.15/0.14)	(0.47/1.50)/(0.23/1.41)
Organic ($\mu g\ m^{-3}$)	(0.04/0.03)/(0.00/0.03)	(0.11/0.12)/(0.09/0.14)	(0.27/0.25)/(0.28/0.31)	(0.95/0.61)/(0.77/1.28)
Sulfate ($\mu g\ m^{-3}$)	(0.01/0.01)/(0.00/0.01)	(0.03/0.04)/(0.03/0.03)	(0.07/0.08)/(0.08/0.08)	(0.18/0.20)/(0.29/0.23)
CH_4 (ppb)	(0/0)/(0/0)	(0/1)/(1/1)	(1/2)/(2/3)	(8/6)/(10/9)
CO_2 (ppm)	(0.0/0.0)/(0.0/0.0)	(0.0/0.1)/(0.1/0.1)	(0.1/0.2)/(0.3/0.4)	(0.6/0.5)/(1.3/1.3)
CO (ppb)	(2.6/2.4)/(2.6/2.6)	(3.0/3.0)/(3.0/3.3)	(3.3/3.3)/(3.5/3.9)	(5.5/4.1)/(7.2/5.7)
O_3 (ppb)	(0.7/0.7)/(0.7/0.8)	(0.9/1.0)/(0.9/1.0)	(1.1/1.2)/(1.2/1.3)	(2.6/2.6)/(1.6/2.2)
H_2O (ppm)	(118/35)/(48/38)	(203/287)/(174/241)	(369/560)/(331/707)	(1065/1400)/(1052/2116)
wind ($m\ s^{-1}$)	(1.1/0.3)/(1.3/1.3)	(1.1/0.6)/(1.3/1.3)	(1.2/1.0)/(1.3/1.3)	(1.2/1.2)/(1.3/1.3)
θ (K)	(0.0/0.0)/(0.0/0.0)	(0.1/0.1)/(0.0/0.1)	(0.1/0.1)/(0.1/0.2)	(0.3/0.6)/(0.5/0.4)

Table S7. Statistics for selected aerosol, gaseous, and meteorological variables measured during ACTIVATE 2020 flights. Statistics are calculated for adjacent BCB legs for cloud ensembles in the first two data columns. The rightmost three columns report correlation statistics between the two BCB legs in cloud ensembles, including separation for winter and summer seasons.

BCB1/BCB2			(all,summer,winter)		
Parameter	Median	no. pairs	Slope	R^2	MARD
Altitude (m)	777/809	91/91	-	-	-
$N_{a,>3nm}$ (cm^{-3})	1585/1618	90/91	(0.76,0.77,0.75)	(0.64,0.79,0.55)	(0.22,0.14,0.28)
$N_{a,>10nm}$ (cm^{-3})	1246/1290	90/91	(0.81,0.79,0.82)	(0.68,0.80,0.59)	(0.22,0.14,0.27)
$N_{a,100-1000nm}$ (cm^{-3})	292/293	90/91	(0.86,0.89,0.74)	(0.83,0.93,0.56)	(0.17,0.12,0.21)
$N_{a,>1000nm}$ (cm^{-3})	0.87/0.84	90/91	(0.91,0.92,0.84)	(0.86,0.93,0.46)	(0.22,0.15,0.27)
$N_{a,>3000nm}$ (cm^{-3})	0.41/0.42	88/87	(0.75,0.76,0.48)	(0.59,0.72,0.17)	(0.30,0.25,0.34)
Organic (μg m^{-3})	0.95/0.96	89/90	(0.90,0.89,0.81)	(0.92,0.91,0.58)	(0.33,0.30,0.36)
Sulfate (μg m^{-3})	0.79/0.82	89/90	(0.95,0.92,0.94)	(0.89,0.86,0.83)	(0.18,0.17,0.19)
CH_4 (ppb)	1974/1973	76/76	(0.93,0.92,0.94)	(0.89,0.91,0.84)	(0.00,0.00,0.00)
CO_2 (ppm)	417.4/416.8	76/76	(0.99,0.95,0.93)	(0.98,0.95,0.89)	(0.00,0.00,0.00)
CO (ppb)	129.1/129.8	76/76	(0.96,0.92,0.93)	(0.96,0.94,0.87)	(0.02,0.03,0.02)
O_3 (ppb)	41.7/42.1	91/91	(0.97,0.97,0.94)	(0.96,0.96,0.88)	(0.03,0.05,0.02)
H_2O (ppm)	10800/10745	91/91	(0.97,0.97,0.93)	(0.98,0.97,0.94)	(0.07,0.05,0.09)
wind ($m\,s^{-1}$)	8.2/7.9	91/91	(0.93,0.90,0.95)	(0.89,0.85,0.91)	(0.14,0.12,0.14)
σ_{wind} ($m\,s^{-1}$)	0.8/0.7	89/90	(0.83,0.78,0.87)	(0.74,0.60,0.76)	(0.20,0.26,0.17)
θ (K)	289.0/288.8	91/91	(0.98,1.01,0.96)	(0.99,0.98,0.96)	(0.00,0.00,0.00)

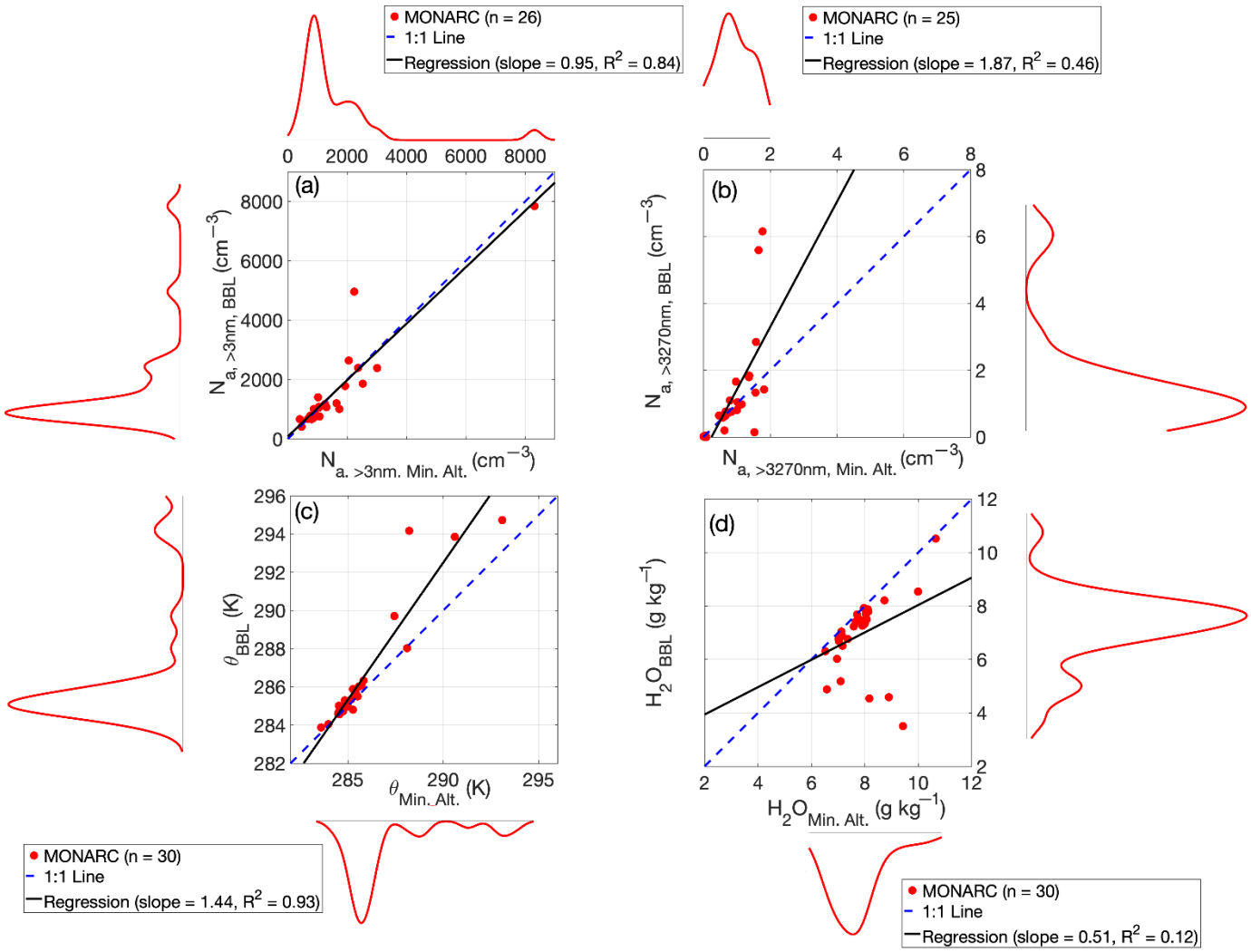

Figure S1. Scatterplots of leg-mean values for selected variables measured in BBL and Min. Alt. legs in clear ensembles during 2019 MONARC flights. The plots on the sides are marginal distributions based on Kernel density estimation.

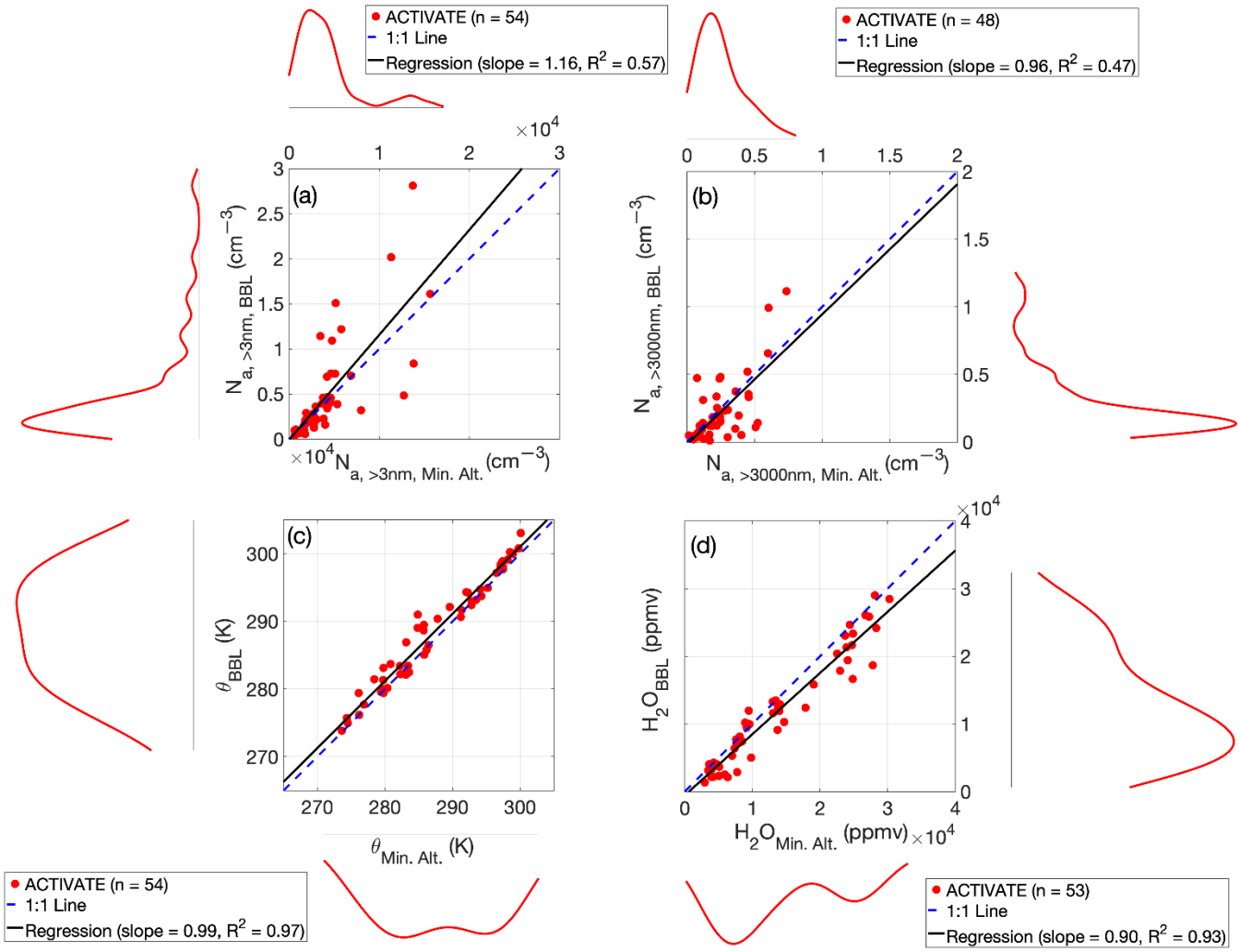

Figure S2. Scatterplots of leg-mean values for selected variables measured in BBL and Min. Alt. legs in clear ensembles during 2020 ACTIVATE flights. The plots on the sides are marginal distributions based on Kernel density estimation.

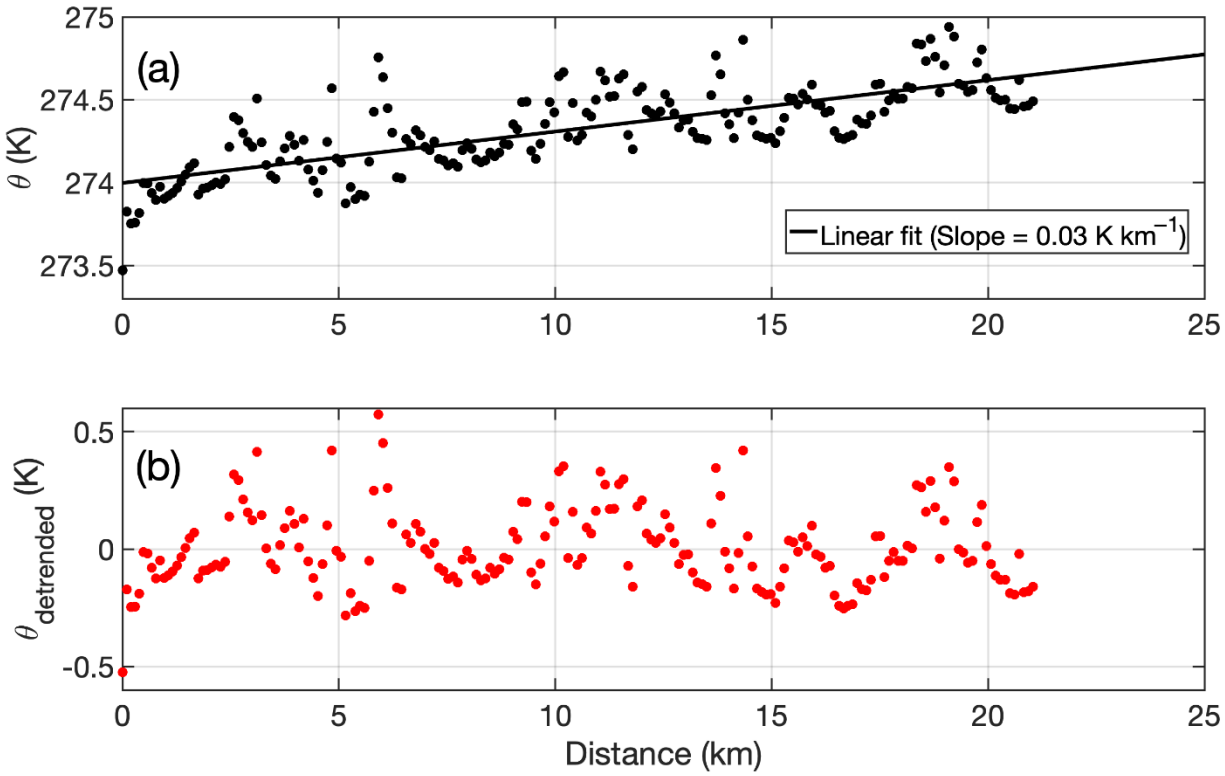

Figure S3. Example of removing the linear trend across an individual level leg. (**a**) Raw data for potential temperature for the Min. Alt. let in ACTIVATE research flight 4 on 21 February 2020 between UTC 19:14:58 and 19:18:17. (**b**) Detrended data for the same Min. Alt. leg.

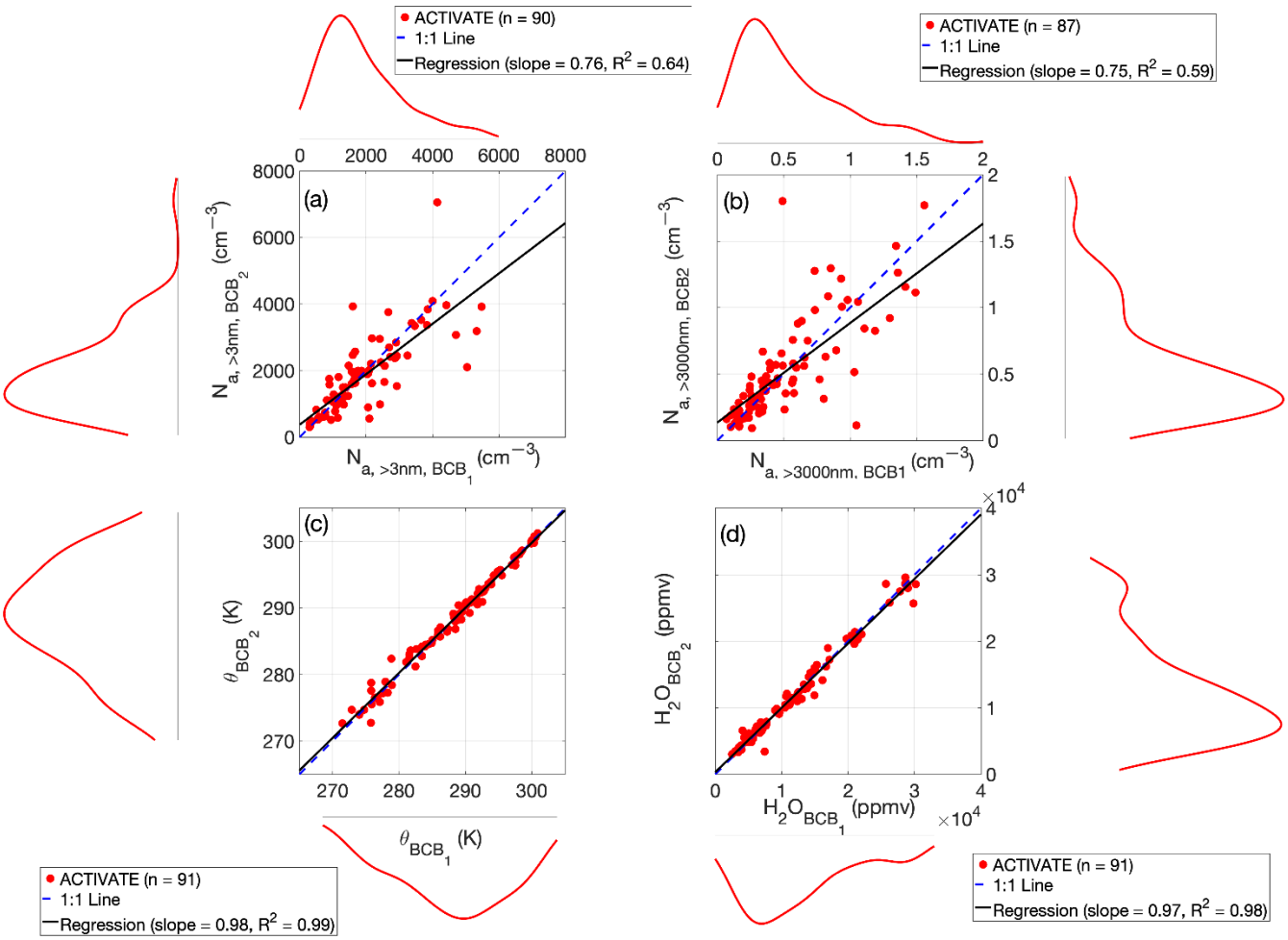

Figure S4. Comparison between two consecutive BCB legs for selected variables measured in cloud ensembles during 2020 ACTIVATE flights. Markers represent leg-mean values.